Percentage change patterns in cloud fraction effectively constrain global cloud feedback

Jian Ma[1]*, Jing Feng[1], In-Sik Kang[2,1], Matthew Collins[3], Masahiro Watanabe[4], Jianping Li[5,6] & Yinding Zhang[7]

[1]*School of Oceanography, Shanghai Jiao Tong University, Shanghai, China*

[2]*State Key Laboratory of Satellite Ocean Environment Dynamics, Second Institute of Oceanography, Ministry of Natural Resources, Hangzhou, Zhejiang, China*

[3]*College of Engineering, Mathematics and Physical Sciences, University of Exeter, Exeter, UK*

[4]*Atmosphere and Ocean Research Institute, University of Tokyo, Kashiwa, Chiba, Japan*

[5]*Frontiers Science Center for Deep Ocean Multi-spheres and Earth System/Key Laboratory of Physical Oceanography/Academy of the Future Ocean, Ocean University of China, Qingdao, Shandong, China*

[6]*Laboratory for Ocean Dynamics and Climate, Pilot Qingdao National Laboratory for Marine Science and Technology, Qingdao, Shandong, China*

[7]*School of Industrial Engineering, Purdue University, West Lafayette, IN, USA*

Nature

20 February 2022, submitted

***Corresponding author:** Jian Ma, School of Oceanography, Shanghai Jiao Tong University, Shanghai 200030, P. R. China. e-mail: Jian.Ma@SJTU.edu.cn

Extended Data Figure Legends

Extended Data Figure 1 | Intermodel scatterplot between total cloud radiative feedback (W m^{-2} K^{-1}) and that by type (color, sum in black) in (a) shortwave, (b) longwave, and (c) net radiation. For each feedback, symbols mark intermodel anomalies from the ensemble-mean values represented by the dashed lines. The feedback variances (exclusive R^2 in Methods, %) explained by specific cloud types are listed with the slopes in the corresponding regressions. Here we use the monthly-mean cloud radiative kernels, and 30 CMIP6 simulations normalized by the global-mean surface air warming.

Extended Data Figure 2 | Spatial correlations (solid lines) between SST patterns T^* and (a) percentage change Δ, and (b) fraction change δC in total (black) and specific types (color) of clouds from individual models. The dashed lines represent the ensemble means of the solid lines, and their values are marked with intermodel spreads. Here we use the 30 CMIP6 simulations normalized by the global-mean surface (air) warming.

Extended Data Figure 3 | Same as Figure 2, but calculated with the MODIS observations during 2003-2020. In this period, the global-mean surface (air) warming is too week so that the normalized changes between the last and first 9-year-means are divided by 10 for better comparisons.

Extended Data Figure 4 | Same as Figure 3, but calculated with the MODIS observations. During this period, the global-mean surface warming is too week so that the normalized changes are divided by 10 for better comparisons.

Extended Data Figure 5 | Horizontal distribution (left) and zonal mean (right) of the fractional cloud kernels (γK, W m^{-2} %$^{-1}$) calculated with simulated cloud climatology

for the tropical (a) shortwave, (b) longwave, and (c) net radiation. After summing throughout optical depths, a vertical sum is performed for the left panel, and a zonal mean for the right. The ensemble means are shown in shading, and intermodel spreads in contours (contour interval: 0.05 W m^{-2} $\%^{-1}$). The dashed lines split cloud types in altitude (440 and 680 hPa). Here, the monthly-mean cloud radiative kernels are multiplied by cloud climatology from 30 CMIP6 simulations, to calculate spatial weights for SST pattern effect.

Extended Data Figure 6 | Same as Extended Data Figure 5, but calculated with the observed cloud climatology from MODIS during 2003-2020.

Extended Data Figure 7 | Intermodel SVD Mode 1 between T^* (K) and scaled anomalous percentage change (Δ', %) in (a, g) high, (b, h) middle, and (c, i) low clouds, and tropical zonal means of the (d) Pacific, (e) Atlantic, and (f) Indian Ocean. In the horizontal distributions (**a**-**c**, **g**-**i**), Δ' is shown in shading, T^* is presented by contours (contour interval: 0.02 K). In the tropical zonal means (**d**-**f**), the left panel shows cloud-type dispatches compared with T^*, and the right panel includes the fractional net cloud kernel (contours, W m^{-2} $\%^{-1}$; contour interval: 0.05 W m^{-2} $\%^{-1}$). The tropical results are illustrated in (**a**-**f**), and the extratropics in (**g**-**i**). Here we use the 30 CMIP6 simulations normalized by the global-mean surface (air) warming.

Extended Data Figure 8 | Same as Extended Data Figure 7, but for the scaled SVD Mode 4. This resembles the original Mode 2 (18%) without the initial constraint.

Extended Data Figure 9 | Cumulative variance (%) of substituted cloud feedback anomalies associated with ensemble-mean fractional kernel explained by the leading SVD modes. The cumulative variance (exclusive R^2 in Methods) was calculated with reordered modes according to their individual variances. Here we use the monthly-mean cloud radiative kernels, and 30 CMIP6 simulations normalized by the global-mean surface (air) warming.

Extended Data Figure 10 | Intermodel scatterplot between substituted feedback (W m^{-2} K^{-1}) and its factor contributions (color, sum in black) in the attribution framework, Eq. (3), including cumulation of the first 20 SVD modes controlled by SST patterns, residual factors, fractional kernel biases, and the nonlinear interaction, in (a) total, (b) high, (c) middle, and (d) low clouds. For each factor, symbols mark intermodel anomalies from the ensemble-mean values represented by the dashed lines. Variances (exclusive R^2 in Methods, %) of cloud feedback explained by specific factors are listed with the slopes in the corresponding regressions. Here we use the monthly-mean cloud radiative kernels, and 30 CMIP6 simulations normalized by the global-mean surface (air) warming.

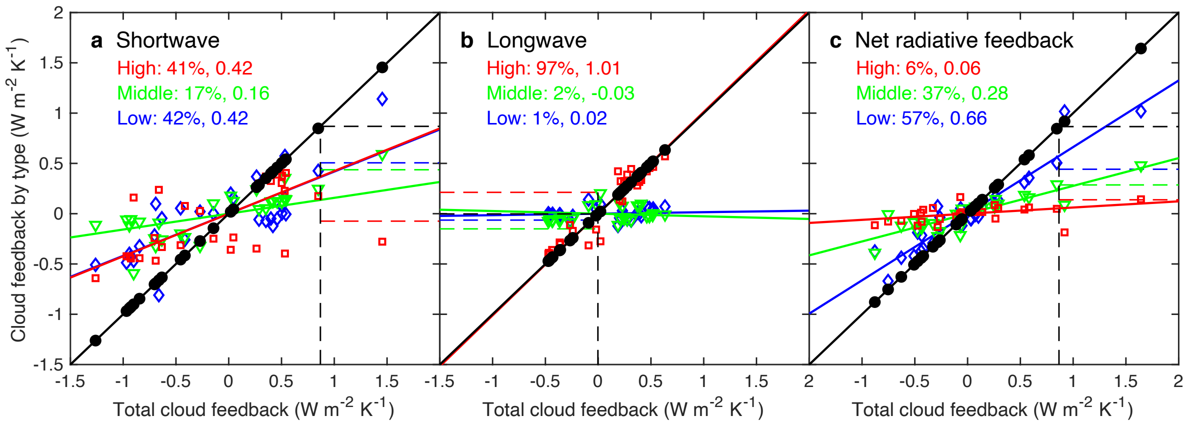

Extended Data Figure 1 | Intermodel scatterplot between total cloud radiative feedback (W m^{-2} K^{-1}) and that by type (color, sum in black) in (a) shortwave, (b) longwave, and (c) net radiation. For each feedback, symbols mark intermodel anomalies from the ensemble-mean values represented by the dashed lines. The feedback variances (exclusive R^2 in Methods, %) explained by specific cloud types are listed with the slopes in the corresponding regressions. Here we use the monthly-mean cloud radiative kernels, and 30 CMIP6 simulations normalized by the global-mean surface air warming.

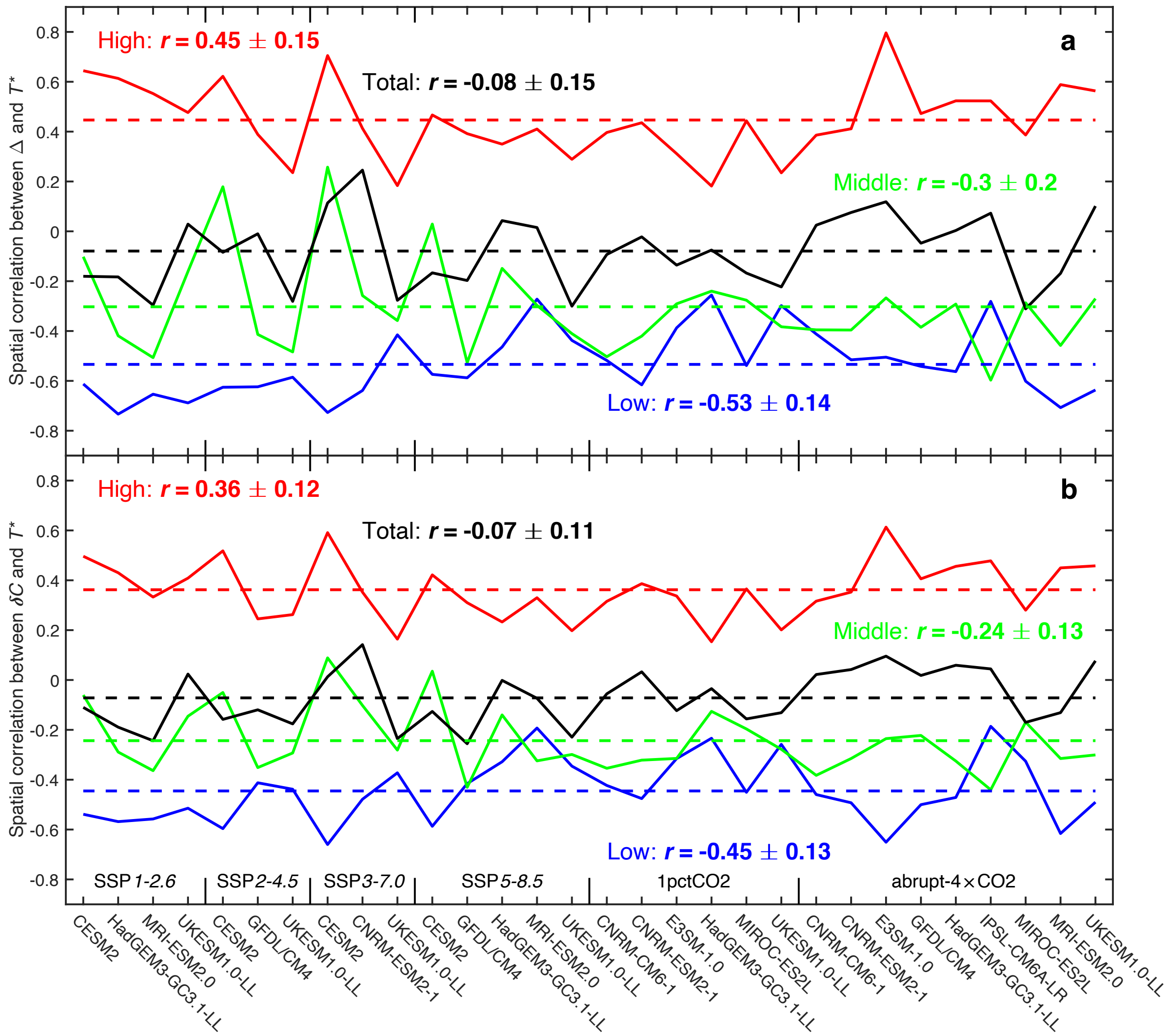

Extended Data Figure 2 | Spatial correlations (solid lines) between SST patterns T^* and (a) percentage change Δ, and (b) fraction change δC in total (black) and specific types (color) of clouds from individual models. The dashed lines represent the ensemble means of the solid lines, and their values are marked with intermodel spreads. Here we use the 30 CMIP6 simulations normalized by the global-mean surface (air) warming.

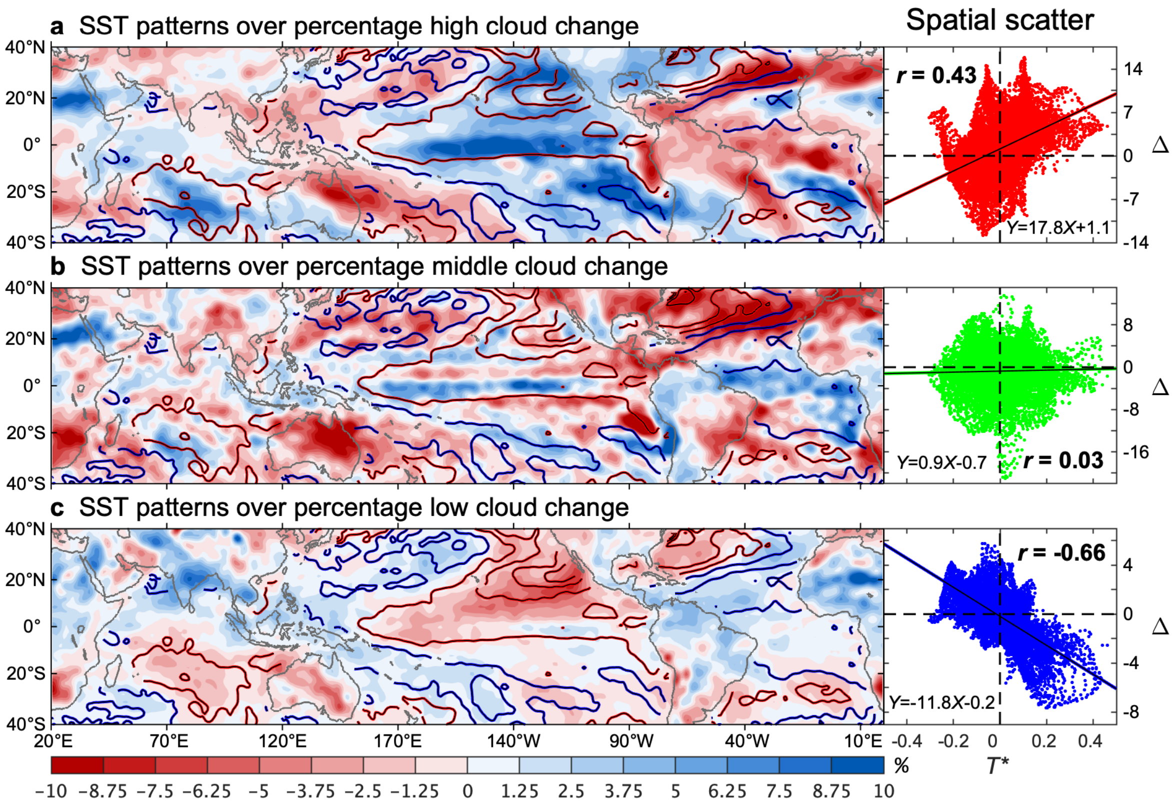

Extended Data Figure 3 | Same as Figure 2, but calculated with the MODIS observations during 2003-2020. In this period, the global-mean surface (air) warming is too week so that the normalized changes between the last and first 9-year-means are divided by 10 for better comparisons.

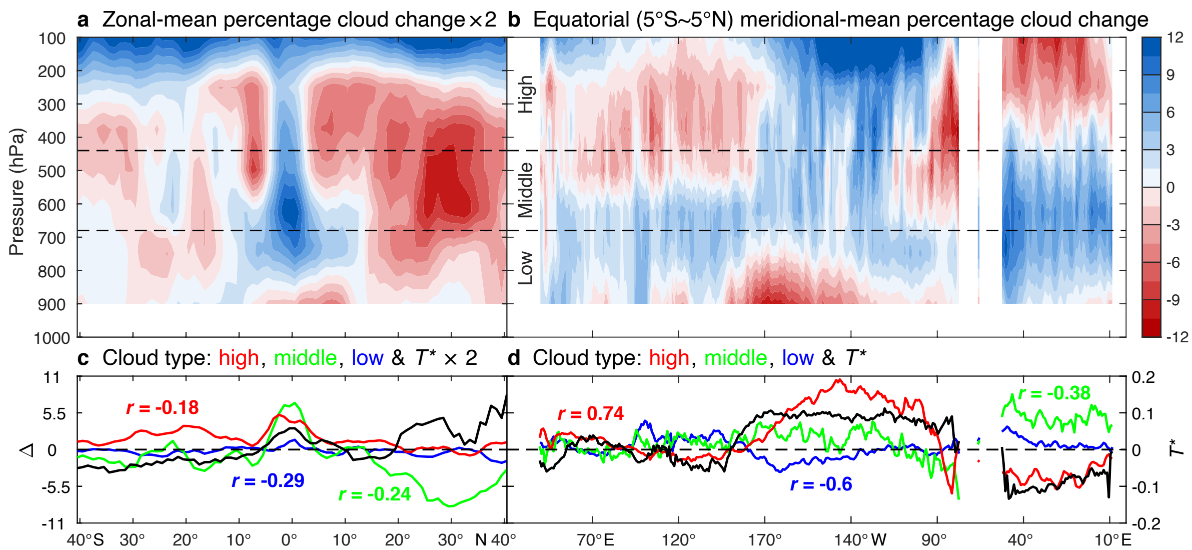

Extended Data Figure 4 | Same as Figure 3, but calculated with the MODIS observations. During this period, the global-mean surface warming is too week so that the normalized changes are divided by 10 for better comparisons.

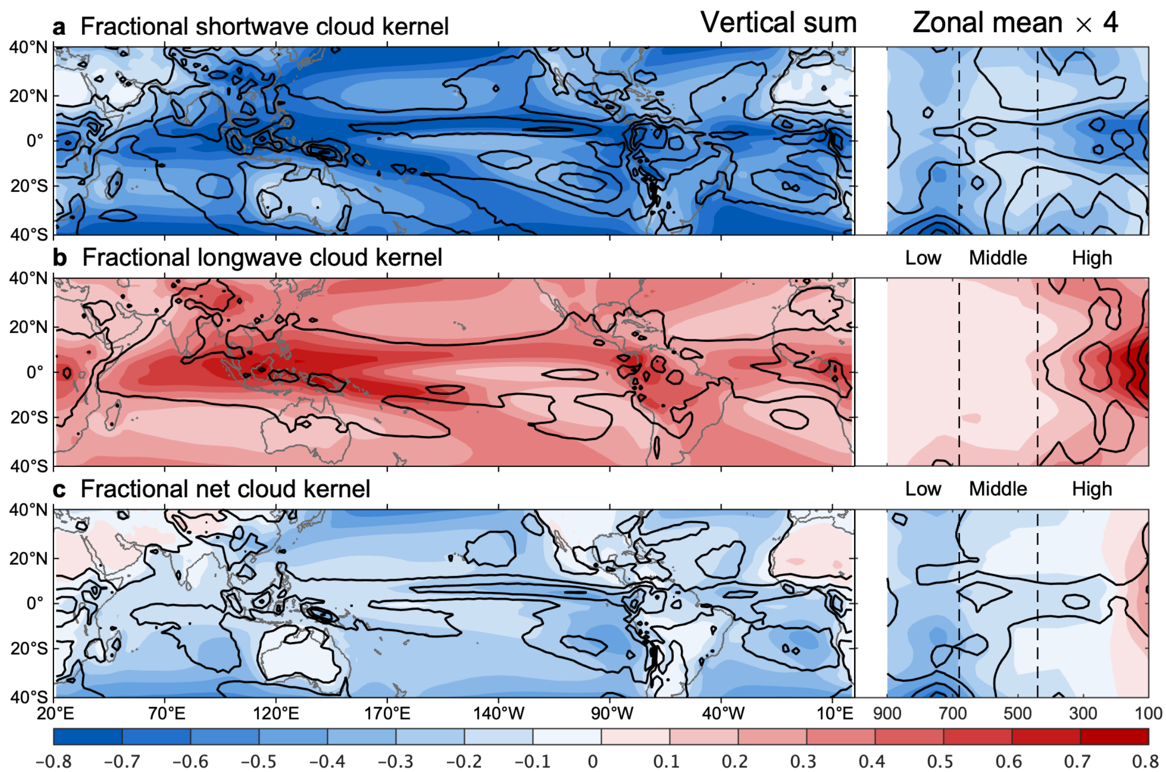

Extended Data Figure 5 | Horizontal distribution (left) and zonal mean (right) of the fractional cloud kernels (γK, W m^{-2} %$^{-1}$) calculated with simulated cloud climatology for the tropical (a) shortwave, (b) longwave, and (c) net radiation. After summing throughout optical depths, a vertical sum is performed for the left panel, and a zonal mean for the right. The ensemble means are shown in shading, and intermodel spreads in contours (contour interval: 0.05 W m^{-2} %$^{-1}$). The dashed lines split cloud types in altitude (440 and 680 hPa). Here, the monthly-mean cloud radiative kernels are multiplied by cloud climatology from 30 CMIP6 simulations, to calculate spatial weights for SST pattern effect.

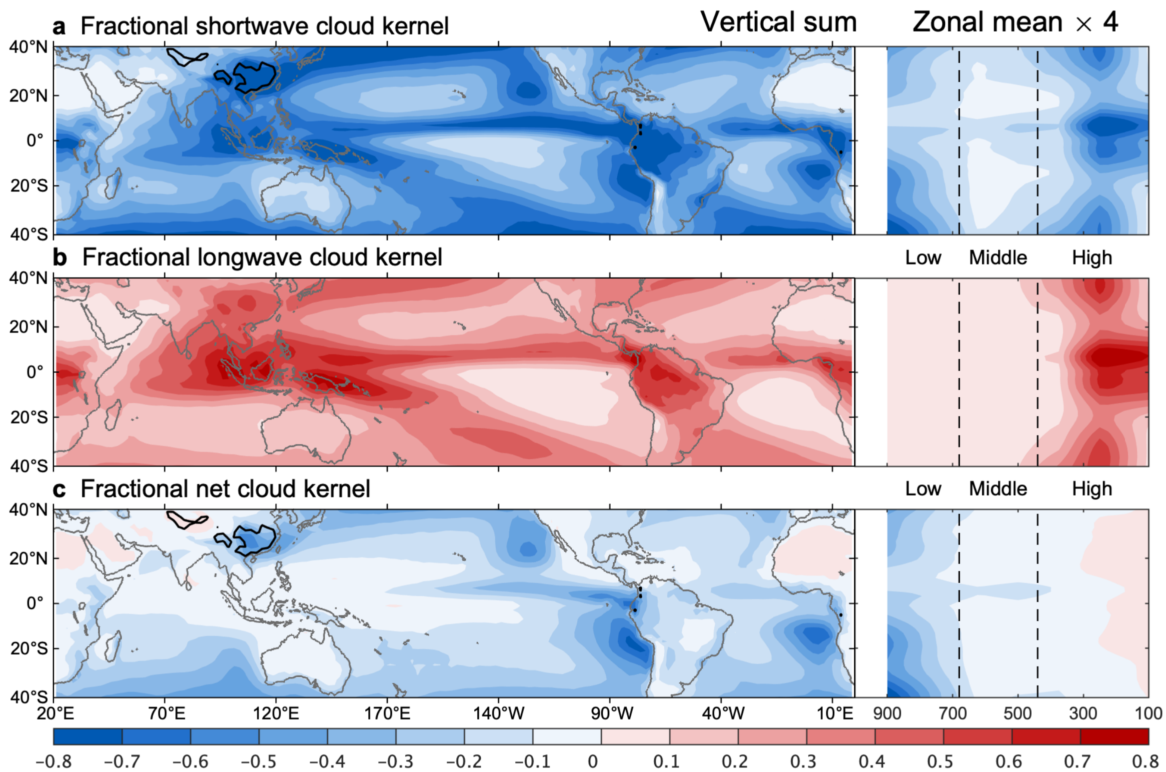

Extended Data Figure 6 | Same as Extended Data Figure 5, but calculated with the observed cloud climatology from MODIS during 2003-2020.

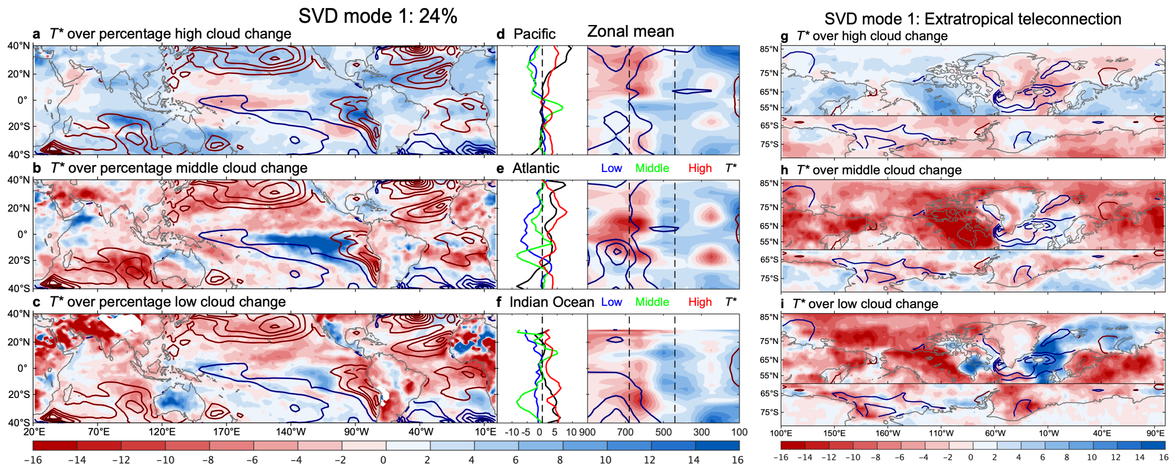

Extended Data Figure 7 | Intermodel SVD Mode 1 between T^* (K) and scaled anomalous percentage change (Δ', %) in (a, g) high, (b, h) middle, and (c, i) low clouds, and tropical zonal means of the (d) Pacific, (e) Atlantic, and (f) Indian Ocean. In the horizontal distributions (**a**-**c**, **g**-**i**), Δ' is shown in shading, T^* is presented by contours (contour interval: 0.02 K). In the tropical zonal means (**d**-**f**), the left panel shows cloud-type dispatches compared with T^*, and the right panel includes the fractional net cloud kernel (contours, W m^{-2} %$^{-1}$; contour interval: 0.05 W m^{-2} %$^{-1}$). The tropical results are illustrated in (**a**-**f**), and the extratropics in (**g**-**i**). Here we use the 30 CMIP6 simulations normalized by the global-mean surface (air) warming.

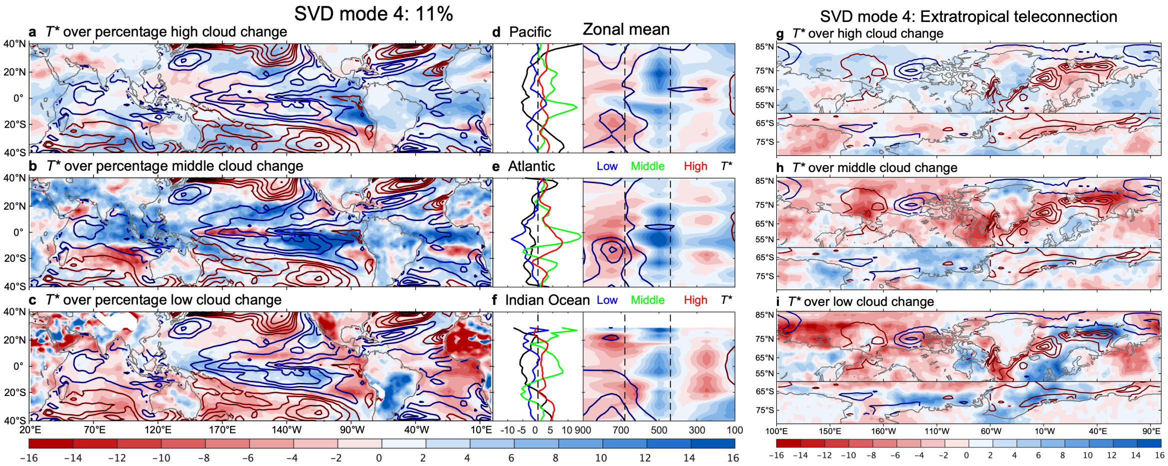

Extended Data Figure 8 | Same as Extended Data Figure 7, but for the scaled SVD Mode 4. This resembles the original Mode 2 (18%) without the initial constraint.

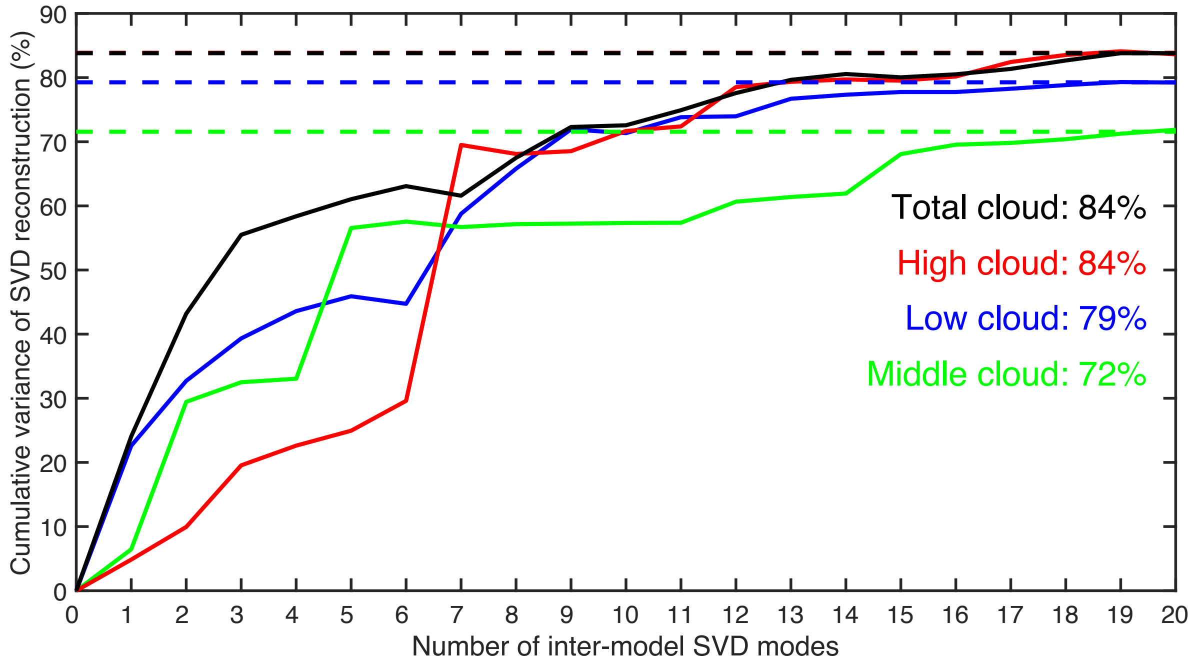

Extended Data Figure 9 | Cumulative variance (%) of substituted cloud feedback anomalies associated with ensemble-mean fractional kernel explained by the leading SVD modes. The cumulative variance (exclusive R^2 in Methods) was calculated with reordered modes according to their individual variances. Here we use the monthly-mean cloud radiative kernels, and 30 CMIP6 simulations normalized by the global-mean surface (air) warming.

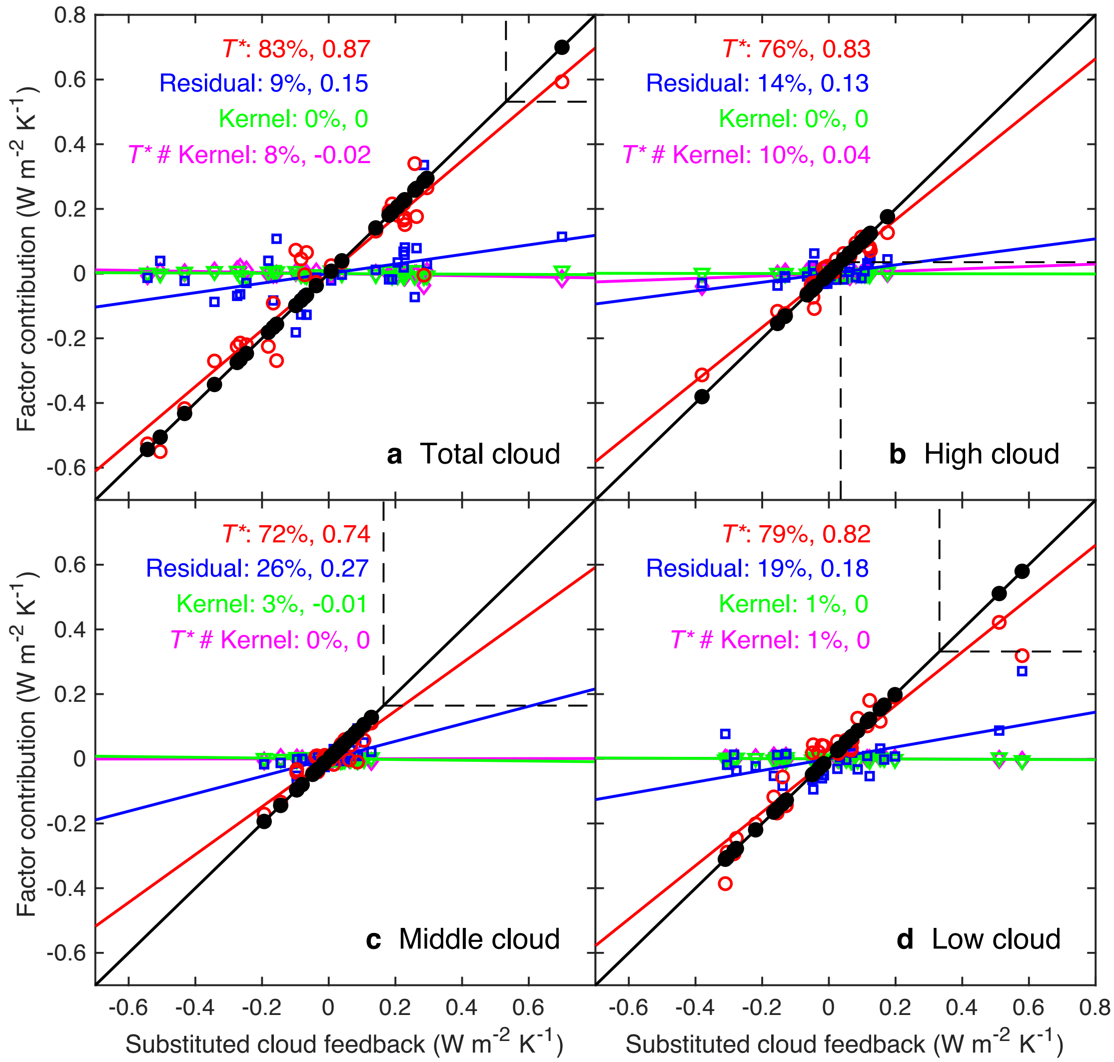

Extended Data Figure 10 | Intermodel scatterplot between substituted feedback (W m^{-2} K^{-1}) and its factor contributions (color, sum in black) in the attribution framework, Eq. (3), including cumulation of the first 20 SVD modes controlled by SST patterns, residual factors, fractional kernel biases, and the nonlinear interaction, in (a) total, (b) high, (c) middle, and (d) low clouds. For each factor, symbols mark intermodel anomalies from the ensemble-mean values represented by the dashed lines. Variances (exclusive R^2 in Methods, %) of cloud feedback explained by specific factors are listed with the slopes in the corresponding regressions. Here we use the monthly-mean cloud radiative kernels, and 30 CMIP6 simulations normalized by the global-mean surface (air) warming.